RESEARCH ON THE SYSTEM CONSTRUCTION OF DISASTER-EXPLORATION UNMANNED VEHICLE

[1]JIA-HORNG YANG, [2]DING-YU CHEN, [3]BO-KAI HU, [4]PO-JEN TU

[1,2,3]Electrical and Electronic Engineering, CCIT, National Defense University
E-mail: yang.jiahorng@gmail.com, kaieonrsi@gmail.com, mine814285@gmail.com

Abstract - The main purpose of this study is to establish anomnidirectional, stable unmanned vehicle (UV) system that integrates the mecanumwheel and robotic arm based on sensors for disaster exploration. Firstly, according to the task requirements, we set up the sensor module, core control module, motor drive module, remote control module, and robotic arm module. We applied the dynamic information of the vehiclecollected by the sensor mudule to help establish the more accurate math models of the unmanned vehicle and robotic arm system that will facilitate the subsequent designs of the smooth controllers. On the vehicle structure, the feature of the mecanumwheelenables the UVto travel flexibly in a confined space for disaster exploration. Finally, through the interfaces of the remote monitoring and control system, core control moduleeffectively integrated the software and hardware architectures of the UV system that enabled to stably and accurately control the robotic arm to safely and efficientlydispose explosives materials. Therefore, UV could smoothly complete the tasks of the disaster exploration and explosive disposition.

Keywords - Disaster exploration, Unmanned vehicle, Robotic arm

I. INTRODUCTION

In recent years, the rapid changes in the global environment and climate caused many disasters frequently. According to statistics, there are more than 200 earthquakes and 3.4 invasive typhoons per year in Taiwan, since Taiwan is located in the pacific rim of fire
and the semi-tropical monsoon climate area. Looking back at the disasters in Taiwan during the past few years, from the 921 earthquake in 1999, Typhoon Xangsane in 2000, Typhoon Nari in 2001, and Typhoon Morakotin 2009, many natural disasters have caused the many casualties and destructions. Besides, according to the report of the "Natural Disaster Hotspot: Global Risk Analysis" in 2005, Taiwan may be the most vulnerable region on the planet. There are about 73% land and people exposed to three or more risk factors for natural disasters[1].
On the 11th March 2011, a strong earthquake with a magnitude of 9 on the Richter scale hit the northeastern region of Japan and caused a combination disaster of the tsunami and the pollution of the nuclear radiation. This combined disaster is the most serious natural disasterin Japan, and caused the heavy casualties in areas such as Iwate, Miyagi, and Fukushima. In this disaster, due to the harsh environment, the disaster relief was not easy to enter the disaster area, and this situation expanded the casualties. This reality has also raised the motivation for us to research and develop the disaster exploration UV. Therefore, throw a sprat to catch a whale. We actively invested this research for disaster relief and hope it could be an example of a good deed for others to follow. Then, through the researches and developments of the UVs and concerted efforts,the casualties of disasterwill be reduced in the future. This is the motivation of this paper.
In addition, the main body of the UV system in this research is the Unmanned Ground Vehicle (UGV), also known as self-propelled vehicle. Currently, there are many applications in various fields, and according to the different functions, can be divided into object tracking [1,2], target identification [3],obstacle avoidance [4-6], and path following [7-9], etc.; however, perhaps the characteristics that no need personnel driving of the UVs. It causes that not so much research discuss how to keep the features of "driving safety" and "stable controlling" [1-13]currently.
From the standpoint of the system integration and controller design, the performance of a system must be based on the stable response of the entire system. For this reason, this article also committed on currently the less of research of driving safety and stable controlling of UV.Imagine that an UV that can track the target, avoid the obstacle, follow the path, if it can also have both the features of driving safety and stable controlling when traveling or steering. These characteristics not only can reduce the vehicle vibrations to extend the life of components but also can help carry out special missions like ammunition transportation, precision substance transportation, and explosive disposition. In addition, the robotic arm module of the UV system is used to dispose explosives materials. Finally, the design of this study can be applied to the disaster exploration and explosive disposition in the disaster area, especially some disaster areas that are extremely harmful to the casualties. Through this study, we hopethe casualties of disaster will be reduced in the future. Therefore, this is a worthwhile issue.

II. UNMANNED VEHICLE ARCHITECTURE

In this study, the hardware architecture of the disaster-exploration UVsystem is divided into two parts: the unmanned groundvehicle (UGV) and the

robotic armmodule. The skeIetonintroduction is highlighted below.

A. UGV ARCHITECTURE

In this study, according to the requirement of the disaster exploration, we planned and set up the UGV architecture (seen as Fig.1). The functional integrated module for UGV system includes: (1) Core control module: orionarduino UNO;(2) Sensor module : 3-axis accelerometer and Gyro sender, ultransonicsensor, camera; (3) Motor driver module: high encoder power driver;(4) Remote control module: bluetoothmodule; (5)Roboticarm module: six-axis robotic arm.

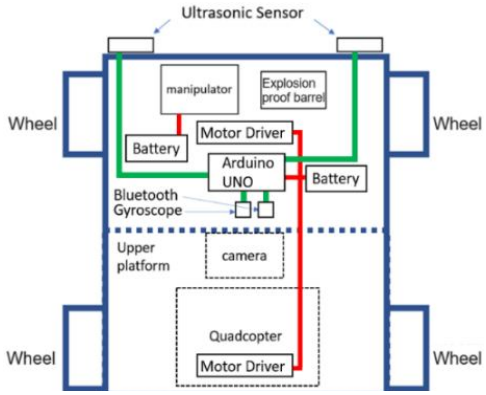


Fig 1. UGV architecture

In addition, considering the inconvenience of driving roads in the disaster area, we changed the original wheels of the UGVto the mecanum wheels (seen as Fig. 2). This modification will be helpful to facilitate the UGV to drive in a narrow space to complete the disaster exploration and explosivetransportation.

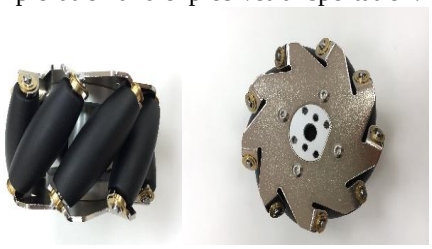


Fig 2. Mecanum Wheel

B. Robotic-Arm ARCHITECTURE

The robot arm mounted on the UV in this study is a six-axis robotic arm (seen Fig. 3). The RobotisDynamixel's AI motor are selected as the motor on the robotic arm (seen as Fig. 4), including the MX-28, MX-64 and MX-106.Among them, MX indicates that the motors are combination of Swiss MAXON motors and Atmemicrocontroller; the number marked behind the motor represents the torque value, such as the MX-28 motor, the number 28 means the static torque of the motor is 28Kg/cm.Besides, the motor of the robotic arm adopts RS-485 serial communication.In addition, considering that the different motor installation positions will result in different force,therefore, proper torque configuration had been planned in advance for motor selections.



Fig 3. Three-axis robotic arm

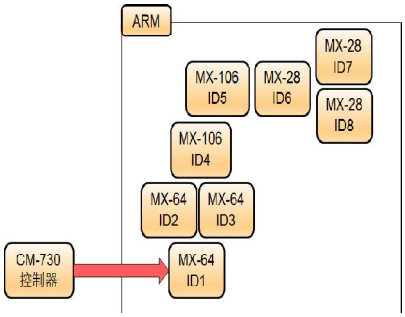


Fig 4. Robotic arm platform

III. ESTABLISHMENT OF THE SYSTEM MODEL

A. The mathmetical model of UGV

The mathematic model of system motion was establishedfrom the known physical characteristics. According to the motion dynamicsof the system and relevant physical formulae, we derived the transfer function between the various inputs and output responses, and then we could establish the mathematic model of the system. However, many real factors affect the system responses that cause the model establishment to become more difficult. Taking our UGV as an example, it's a Four Wheels Steering (4WS)system. When establishingthe mathematical model, firstly, the general method is to ignore the unimportant factors that have the small impacts on the UGV motion. This step makes model establishment easier. After establishing a rough mathematic model, we applied real motion dynamics collected by the sensor module to compare the originallyrough mathematic modeland verified the system parameters, then we couldobtain a more accurate mathematical model to reduce the negative effect caused by the model error. Fig. 5 is the simplified schematic diagramof UGV motion. The system parameters of UGV motion are also defined in Table 1. Since the equations of UGV motions are public information. We can get the model on the internet or derive the model ourselves. Therefore, due to the page limits, we just listed the final results and state space equation (SSE) of the UGV model (seen as Eq. (1~3))[15]. The detail procedures of deriving the system model can be also found in reference [15] or on the internet. Afterwards, we substituted the real

characteristics of our UGV system into Eq. (3), we could obtain the SSE of the UGV in this study (seen as Eq. (4)).

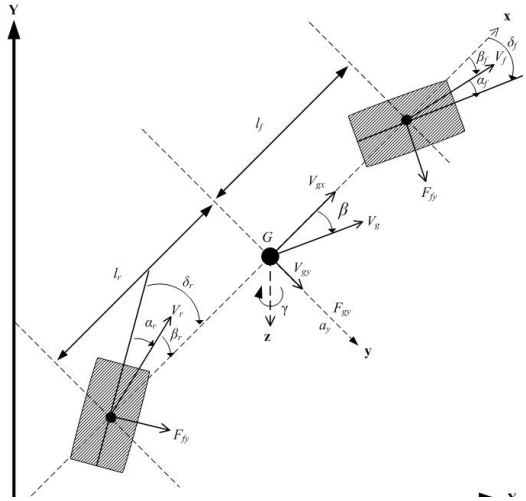


Fig 5. Simplified plane-movement of the UGV model Error! Reference source not found.]

Table1.The system parameters of UGV motion [15]

NAME	PARAMETER DESCRIPTION
L_f	Distance between center of gravity and axle center of front tires
L_r	Distance between center of gravity and axle center of reartires
G	Center of gravity of the UGV
β	Sideslip angle of the center of gravity
β_f	Sideslip angle of center of gravity of the front wheel
β_r	Sideslip angle of center of gravity of the rear wheel
α_f	Sideslip angle of the front wheel
α_r	Sideslip angle of the rear wheel
δ_f	Front-wheel steering angle
δ_r	Rear-wheel steering angle
γ	Yaw rate of the vehicle of the fixed coordinate system
F_{gy}	Side force of the center of gravity
F_{fy}	Side force of the center of gravity of the front wheel
F_{ry}	Side force of the center of gravity of the rear wheel
a_g	Center of gravity acceleration
a_x	Longitudinal acceleration of the center of gravity
a_y	Lateral acceleration of the center of gravity
M	Mass of the UGV
V_g	Speed of UGV's center of gravity
V_{gx}	Vertical speed of the center of gravity
V_{gy}	Lateral speedof the center of gravity
V_f	Speed of the center of gravity of the front wheel
V_r	Speed of the center of gravity of the rear wheel
I_z	Moment of inertia of the Z-axis
K_f	Steering stiffness of the front wheel
K_r	Steering stiffness of the rear wheel

The lateral motion equation:

$$\begin{cases} MV_g(\dot{\beta}+\gamma) = 2K_f \times \left(\delta_f - \beta - \dfrac{\gamma L_f}{V_g}\right) + 2K_r \times \left(\delta_r - \beta + \dfrac{\gamma L_r}{V_g}\right) \\ I_z\dot{\gamma} = L_f \times 2K_f \times \left(\delta_f - \beta - \dfrac{\gamma L_f}{V_g}\right) - L_r \times 2K_r \times \left(\delta_r - \beta + \dfrac{\gamma L_r}{V_g}\right) \end{cases} \quad (1)$$

The yaw motion equation:

$$\begin{cases} \dot{\beta} = \dfrac{-2(K_f + K_r)}{MV_g}\beta + \left(\dfrac{-2(L_fK_f - L_rK_r)}{MV_g^2} - 1\right)\gamma + \dfrac{2K_f}{MV_g}\delta_f + \dfrac{2K_r}{MV_g}\delta_r \\ \dot{\gamma} = \dfrac{-2(L_fK_f - L_rK_r)}{I_z}\beta + \dfrac{-2(L_f^2K_f + L_r^2K_r)}{I_zV_g}\gamma + \dfrac{2L_fK_f}{I_z}\delta_f + \dfrac{-2L_rK_r}{I_z}\delta_r \end{cases} \quad (2)$$

The SSE of the UGV:

$$\begin{cases} \begin{bmatrix} \dot{\beta} \\ \dot{\gamma} \end{bmatrix} = \begin{bmatrix} \dfrac{-2(K_f + K_r)}{MV_g} & \left(\dfrac{-2(L_fK_f - L_rK_r)}{MV_g^2} - 1\right) \\ \dfrac{-2(L_fK_f - L_rK_r)}{I_z} & \dfrac{-2(L_f^2K_f + L_r^2K_r)}{I_zV_g} \end{bmatrix} \begin{bmatrix} \beta \\ \gamma \end{bmatrix} + \begin{bmatrix} \dfrac{2K_f}{MV_g} & \dfrac{2K_r}{MV_g} \\ \dfrac{2L_fK_f}{I_z} & \dfrac{-2L_rK_r}{I_z} \end{bmatrix} \begin{bmatrix} \delta_f \\ \delta_r \end{bmatrix} \\ \begin{bmatrix} \beta \\ \gamma \end{bmatrix} = \begin{bmatrix} 1 & 0 \\ 0 & 1 \end{bmatrix} \begin{bmatrix} \beta \\ \gamma \end{bmatrix} \end{cases} \quad (3)$$

The SSE of the UGV in this study:

$$\begin{cases} \begin{bmatrix} \dot{\beta} \\ \dot{\gamma} \end{bmatrix} = \begin{bmatrix} -6.2079 & -0.6425 \\ 17.7252 & -174.0891 \end{bmatrix} \begin{bmatrix} \beta \\ \gamma \end{bmatrix} + \begin{bmatrix} 2.5866 & 3.6213 \\ 328.6558 & -346.3810 \end{bmatrix} \begin{bmatrix} \delta_f \\ \delta_r \end{bmatrix} \\ \begin{bmatrix} \beta \\ \gamma \end{bmatrix} = \begin{bmatrix} 1 & 0 \\ 0 & 1 \end{bmatrix} \begin{bmatrix} \beta \\ \gamma \end{bmatrix} \end{cases} \quad (4)$$

In additions, 4WSsystem has various control architectures. In this research, we adopted the fixed-ratio control architecture. That means that the steering angle of the rear-wheel always keeps the fixed-ratio to the angle of the front-wheel to yield the stable driving (seen as Eq. (5) and Fig. 6). The main reasons are as follows: (1) The fixed-ratio control architecture is easy to understand and extremely effective; (2) The adjustment of the controller parameters is relatively simple in the fixed-ratio mode. It makes that the software design of the control architecture can be implemented easier in hardware; (3) The fixed-ratio mode control architecture is often applied for generally commercial 4WS.4WS of Nissan and Honda are also based on this control architecture, since the real sensor of the side-slip on the vehicle is too expensive, and the software simulation is also more difficult to compile into Electronic Control Unit (ECU). (4) All dynamics information which we need in fixed-ratio control architecture, including lateral acceleration, yaw rate, and speed of the UGV, can be obtained by the cheaper sensor module. Take this study as the example, the sensor module is much cheaper than the side-slip sensor, so it is easy to implement and suitable for academic researches; (5) The research data and experimental results in the fixed-ratio control architecture is easy to implement to general vehicles. Therefore, it is more practical and has high research value.

$$\delta_r = K_{df}\delta_f \quad (5)$$

Where δ_f and δ_r are the steering angles of the front and rear wheels, respectively. K_{df} is the proportionality constant between δ_f and δ_r.

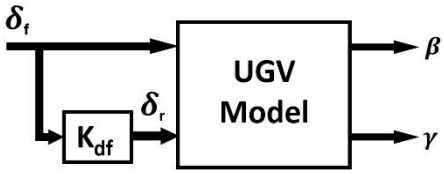


Fig 6. Block diagram of the fixed-ratio mode

We reformulate Eq. (4) as Eq. (6):

$$\begin{cases} \begin{bmatrix} \dot{\beta} \\ \dot{\gamma} \end{bmatrix} = \begin{bmatrix} a_{11} & a_{12} \\ a_{21} & a_{22} \end{bmatrix} \begin{bmatrix} \beta \\ \gamma \end{bmatrix} + \begin{bmatrix} b_{11} & b_{12} \\ b_{21} & b_{22} \end{bmatrix} \begin{bmatrix} \delta_f \\ \delta_r \end{bmatrix} \\ \begin{bmatrix} \beta \\ \gamma \end{bmatrix} = \begin{bmatrix} 1 & 0 \\ 0 & 1 \end{bmatrix} \begin{bmatrix} \beta \\ \gamma \end{bmatrix} \end{cases} \quad (6)$$

Set the differential value in Eq. (6) as zero, we can obtain the proportional constant K_{df}as Eq. (7):

$$K_{df} = \frac{a_{12}b_{21} - a_{22}b_{11}}{a_{22}b_{12} - a_{12}b_{22}} \quad (7)$$

The totally designed architecture of the smooth control steering based on Matlab simulation for the 4WS system

is also shown in Fig. 7. Substituting the proportional constant K_{df} of Eq. (7) into the design architecture in Fig. 7, the 4WS system will maintain better stability when the vehicle is turning.

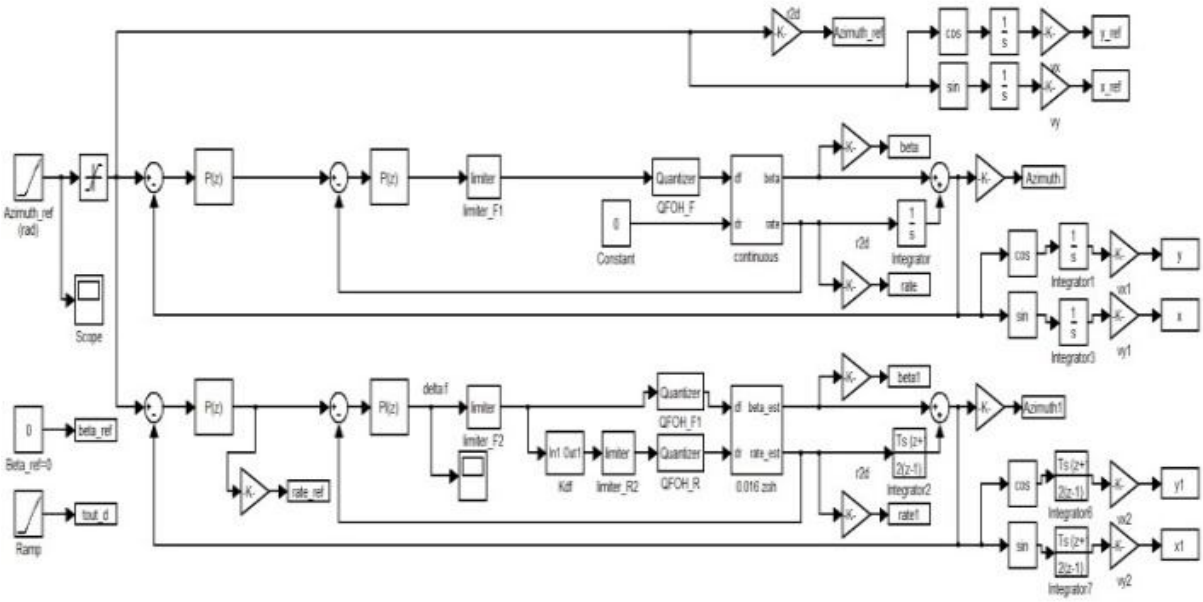


Fig 7. Matlab/Simulink program for 4WS control steering architecture

B. The Mathematical Model of Robotic Arm

The dynamics of the robotic arm is used to describe the relationship among the speed, the acceleration, and the acting force of the robotic arm. Another application is to help establish an ideal motion pattern of the robotic arm. Due to the various architectures of the robotic arms, there are many different motion modes. In this study, we applied the Lagrange's rules to establish the mathematical model of the robotic arm. The sketch is as the following:

If the single-axis robotic arm is shown in Fig. 8, where m is the mass of the robotic arm, r is the distance from the joint to the link, q is the rotation angle of the joint, and τ is the input force of the joint. In order to obtain the Lagrange equation, firstly, we needed to determine the total kinetic energy K and the total potential energy P of the robotic arm (seen as Eq. (8) and Eq. (9)):

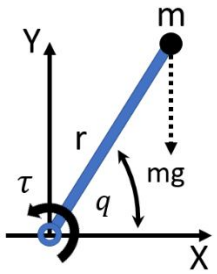


Fig 8. Single-axis robotic arm

$$K = \frac{1}{2}(I + mr^2)\dot{q}^2 \quad (8)$$

$$P = mgr\cos(q) \quad (9)$$

Afterwards, according to the Lagrange rules, we could obtain the Lagrange equation and the dynamic equation as the as Eq. (10) and Eq. (11), respectively:

$$L = K - P = \frac{1}{2}(I + mr^2)\dot{q}^2 - mgr\cos(q) \quad (10)$$

$$(mr^2 + I)\ddot{q} + gmr\cos q = \tau \quad (11)$$

Eq. (11) is the dynamic equation of the single-axis robotic arm. Besides, if one n-axis robotic arm has n joints

and n degrees of freedom, n angles of the n joints are defined as q=(q_1, q_2, q_3,...,q_n). let K and P be the total kinetic energy and the total potential energy of the n joints of the robotic-arm system, respectively. According the Lagrange equation: L = K-P, we can obtain the matrix form of dynamic equation for the multi-degree-of-freedom robotic-arm. If the robotic arm is 2 degrees of freedom, that also means n=2, then we can obtain the dynamic equation of the 2-degree-of-freedom, such as Eq. (12):

$$D(q)\ddot{q}+C(q,\dot{q})\dot{q} + G(q) = \tau \quad (12)$$

Where $\dot{q}, \ddot{q} \in R$, is the first and second derivative of q, D(q) is the positive matrix of inertial matrix, and$C(q,\dot{q})$ is also an×n matrix. $C(q,\dot{q})$is the Coriolis force and the Centrifugal force, respectively. G(q) is the dynamic vector with the n×1 dimension. For example, Fig. 9 is a schematic diagramof the two-axis robotic arm. Table 2 is the symbol description for Fig. 9：

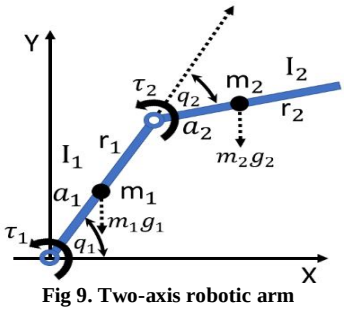


Fig 9. Two-axis robotic arm

Table2.Symbol description for Two-axis Robotic arm

Name	Explanation
τ_1, τ_2	The input force of the joint
a_1, a_2	The distance between the center of mass to its joint
r_1, r_2	The distance between the center of next joint
I_1, I_2	The link length
m_1, m_2	The link mass
q_1, q_2	rotation angle of the Mechanical axis
g_1, g_2	Earth's gravity at the surface of an object

The motion equation of the two-axis robotic arm shown in Fig. 9 is much more complicated than the single-axis robotic arm in Fig. 8, because when operating two or more axes robotic arms, additionally, we should consider the influence of the Coriolis force. Therefore, the procedures for establishing the mathematical model of the two-axis robotic arm are as follows:

Step1. As certain every position and speed for each link of the robotic arm (seen as Eq. (13)~Eq. (16)):

Positions:

$$\begin{bmatrix} x_1 \\ y_1 \end{bmatrix} = \begin{bmatrix} a_1 cosq_1 \\ a_1 sinq_1 \end{bmatrix} \quad (13)$$

$$\begin{bmatrix} x_2 \\ y_2 \end{bmatrix} = \begin{bmatrix} r_1 cosq_1 + a_1 cos\,(q_1 + q_2) \\ r_1 sinq_1 + a_1 sin\,(q_1 + q_2) \end{bmatrix} \quad (14)$$

Speed:

$$\begin{bmatrix} \dot{x}_1 \\ \dot{y}_1 \end{bmatrix} = \begin{bmatrix} -a_1 sinq_1 \\ a_1\ cosq_1 \end{bmatrix} \dot{q}_1 \quad (15)$$

$$\begin{bmatrix} \dot{x}_2 \\ \dot{y}_2 \end{bmatrix} = \begin{bmatrix} -r_1 s_1 - a_2 sin\,(q_1 + q_2) \\ r_1 c_1 + a_2 cos\,(q_1 + q_2) \end{bmatrix} \dot{q}_1 + \begin{bmatrix} -a_2 sin\,(q_1 + q_2) \\ a_2 cos\,(q_1 + q_2) \end{bmatrix} \dot{q}_2 \quad (16)$$

Step2. Calculate the total kinetic energy K of the two-axis robotic arm (seen as Eq. (17), Eq. (18)):

$$K_T = K_1 + K_2 \quad (17)$$

$$K_T = \frac{1}{2}\begin{pmatrix} I_1 + I_2 + m_1 a_1^2 \\ +m_2(r_1^2 + a_2^2 + 2r_1 a_2 cosq_2) \end{pmatrix} \dot{q}_1^2 \quad (18)$$

$$+\frac{1}{2}(I_2 + m_2 a_2^2)\dot{q}_2^2$$
$$+\left(I_2 + m_2(a_2^2 + r_1 a_2 cosq_2)\right)\dot{q}_1\dot{q}_2$$

Step3. Calculate the total potential energy P of the two-axis robotic arm (seen as Eq. (19)):

$$P = gm_1 y_1 + gm_2 y_2 = g\begin{pmatrix}(m_1 a_1 + m_2 r_1)sinq_1 \\ +m_2 a_2 sin\,(q_1 + q_2)\end{pmatrix} \quad (19)$$

Step4. Formulate the Lagrange equations (seen as Eq. (20)):

$$\begin{aligned} L &= K - P \\ &= \frac{1}{2}\begin{pmatrix} I_1 + I_2 + m_1 a_1^2 \\ +m_2(r_1^2 + a_2^2 + 2r_1 a_2 cosq_2)\end{pmatrix}\dot{q}_1^2 \\ &+\frac{1}{2}(I_2 + m_2 a_2^2)\dot{q}_2^2 \\ &+\left(I_2 + m_2(a_2^2 + r_1 a_2 cosq_2)\right)\dot{q}_1\dot{q}_2 \\ &- g\begin{pmatrix}(m_1 a_1 + m_2 r_1)sinq_1 \\ +m_2 a_2 sin\,(q_1 + q_2)\end{pmatrix} \end{aligned} \quad (20)$$

Step5. Find the dynamic equations for each link of the robotic arm (seen as Eq. (21), Eq. (22)):

$$\frac{d}{dt}\frac{\partial L}{\partial \dot{q}_1} - \frac{\partial L}{\partial q_1} = \tau_1 \quad (21)$$

$$\frac{d}{dt}\frac{\partial L}{\partial \dot{q}_2} - \frac{\partial L}{\partial q_2} = \tau_2 \quad (22)$$

Finally, we could obtain the dynamic equations of the two-axis robotic arm (seen as Eq. (23)):

$$\begin{bmatrix} D_{11} & D_{12} \\ D_{21} & D_{22}\end{bmatrix}\begin{bmatrix}\ddot{q}_1 \\ \ddot{q}_2\end{bmatrix} + \begin{bmatrix} C_{11} & C_{12} \\ C_{21} & C_{22}\end{bmatrix}\begin{bmatrix}\dot{q}_1 \\ \dot{q}_2\end{bmatrix} + \begin{bmatrix} G_1 \\ G_2\end{bmatrix} = \begin{bmatrix}\tau_1 \\ \tau_2\end{bmatrix} \quad (23)$$

The motion equations of single-axis and two-axis robotic arms described above can be obtained after derivation. According to the logic and concept, we could also derive the motion equation for six-degree-of-freedom robotic arms. The operating 3-axis robotic arm in this study is six degrees of freedom, and its motion skeleton can be simplified as Fig.10.The dynamic equation of 3-axis robotic arm can be also obtained by repeating the procedures of the dynamic equations for 2-axis robotic arm. Therefore, we could obtain the dynamic equations of 3-axis robotic arm as follows (seen as Eq. (24)~Eq. (27)):

$$D\begin{bmatrix}\ddot{q}_1 \\ \ddot{q}_2 \\ \ddot{q}_3\end{bmatrix} + C\begin{bmatrix}\dot{q}_1 \\ \dot{q}_2 \\ \dot{q}_3\end{bmatrix} + \begin{bmatrix} G_1 \\ G_2 \\ G_3\end{bmatrix} = \begin{bmatrix}\tau_1 \\ \tau_2 \\ \tau_3\end{bmatrix} \quad (24)$$

$$D = \begin{bmatrix} 0.4858 & 0.2757 & 0.0686 \\ 0.2757 & 0.2767 & 0.0686 \\ 0.0686 & 0.0686 & 0.0682\end{bmatrix} \quad (25)$$

$$C = \begin{bmatrix} -0.0122\dot{q}_2\dot{q}_3 & -0.0067\dot{q}_2\dot{q}_3 & -0.00057652\dot{q}_3 \\ -0.0067\dot{q}_2\dot{q}_3 & -0.0012\dot{q}_3 & -0.00057652\dot{q}_3 \\ -0.00057652\dot{q}_3 & -0.00057652\dot{q}_3 & 0\end{bmatrix} \quad (26)$$

$$G = g\begin{bmatrix}-0.0344 \\ -0.08 \\ -0.0052\end{bmatrix} \quad (27)$$

IV. EXPERIMENT RESULT

A. Experiment setting

To verify whether the design and construction of the disaster-exploration UV system is good, we must plan a proper experimental setting to verify the system design before experiment. In the UGV part of the disaster-exploration UV system, since the most unstable situation of the UGV is the moment that UGV encounters the obstacle and makes an emergent steering. Therefore, the experimental setting of the UGV is set that UGV starts from the stationary state and accelerates, and keeps going. Afterwards, UGV encounters the obstacle unexpectedly and makes an emergent turn. The important consideration is that, during the travel, the system designer has to take into account of the stable driving, especially when steering suddenly.Therefore, a rational turning radius needs to be considered in the setting of UGV.In addition, the characteristics of the UGV model, driving speed of the UGV, detection range of the ultrasonic sensor, sampling period of the core control module that is in view of the sensor module to design the stable fixed-ratio control architecturein order to achieve a stably smooth Ackermann steering.Finally, in the UGV part, we verified the design via Matlab simulation.

In the part of the robotic-arm experimental-setting, in view of that, in fact, the explosive disposition requires a very high degree of stability during the gripping and transport. This research is different from the general robotic arm document that is without considering the stable gripping work. In this research, the stability of the explosive gripping must be maintained during the three processes, including to the explosivegripping from the original position, the horizontal transportation from the original position to the vehicle, and the smooth placement when placing the explosive on the stage of the vehicle. Therefore, the control design is necessary to emphasize the accuracy and stability of the robotic arm.

B. Experiment result of the UGV

In this study, we applied the sensor module to collect the dynamic information of the UGV and help correct the derived rough mathematical model (seen as Eq. (3), Eq. (4)), so we could establish a more accurate mathematical model and fixed-ratio control architecture of the UGV.We applied the Matlab/Simulink to verify the goodness degree of the azimuth, yaw rate, and obstacle avoidance trajectories of the UGVdesign. The design results are shown in Fig. 11, Fig. 12, and Fig. 13.The Fig. 11 is the simulation of the azimuth design of the UGV. In Fig. 11, The blue line is the azimuth expectation (Desired Value), the green line represents the condition of the UGV without design (the Without Control Adjustment), and the red line is the system response improved by the fixed-ratio mode controller (Azumuth Controller). From Fig. 11, we could find that although the azimuth response with controller improvement has a slight overshoot (red line). However, it just has a very small error compared with the expectations (blue line), and its response is much better than original UGV system (green line). That means our design really improved the UGV performance and advanced the reaction speed to avoid the obstacle.

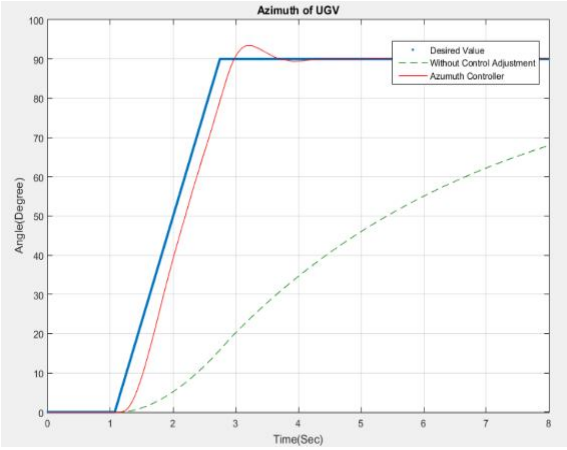


Fig 10 . Comparison of azimuth responses of UGV

In addition, about the vehicle control, the yaw rate is one of the reference indicators for judging whether the vehicle body is out of balance. Fig. 12 shows the comparisons between the original UGV and the result afterour controller compensation. From Fig. 12, it could be easily found thatwhen makingthe obstacle avoidance steering, the original UGV(green line)could not comply with the steering command (blue line)due to its natural characteristics,it had a significant difference from the expected value. However, after compensating by the fixed-ratio control architecture,the improving UGV response (red line) could reliably follow the control commands (blue line) to obtain the expected driving and turning stability. Therefore, the fixed-ratio control architecturecan effectively improve the handling and the flexibility of UGV.

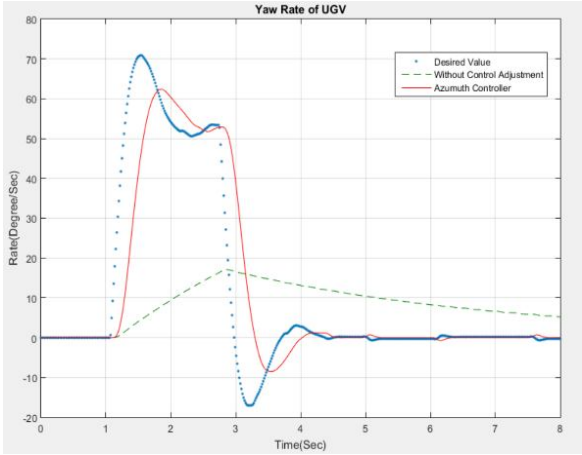


Fig 11. Comparison of yaw-rate response of UGV

Fig. 13 is the driving-path comparison of the original and compensated UGV. It is obviously that the original UGV couldnot perform effective and immediate turning for the obstacle avoidance(green line) due to its under-steer property when encountering the hindrance. This response is very dangerous and will leads to the risk.However, The UGVcompensated through the fixed-ratio control architecture could improve the travel path according to the obstacle position and made the UGV more efficient and quicker in steering(red line) to achieve the goal of obstacle avoidance with a the 90-degree turn (blue line). This result confirms that the fixed-ratio control architecture in this study indeedimproved the UGV performance and advanced the handling and flexibility of the UGV to ensure the high stability when self-driving.

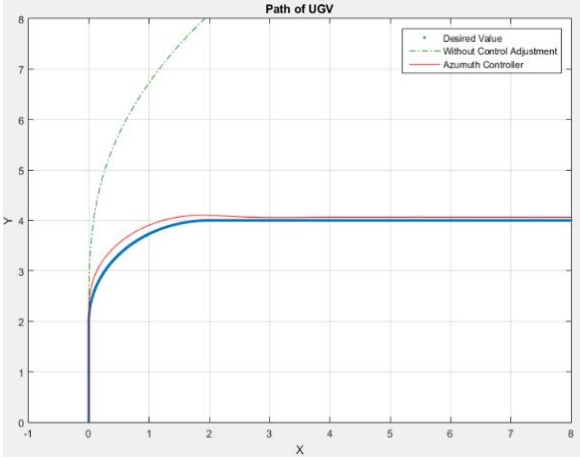


Fig 12. Comparison of driving path of UGV

C. Experimental Verification for Explosive Disposition of Robotic-Arm Design

When the operator discovers explosives through the ultrasonic or web cameras, UGV will stop at proper location that the robotic arm can grip the explosive easily. At that time, operator will switch on the stable gripping mode for explosive disposition. The stable gripping mode of the robotic arm in this study is divided into 3 processes. Every process must keep the same horizontal lever to maintain the stability of the explosive. The first step isthe explosive gripping from the original position of the explosive. When gripping and lifting up the explosive, the designed robotic arm acted slowly and always remained horizontal level of the explosive to avoid the burst (seen as Fig. 14). The second processis the explosive transportation from the original position to the vehicle. During this process, the key element of the robotic-armdesign is toremain the horizontal level of the translational motion (seen as Fig. 15). The final step of the explosive dispositionis the smooth placement when placing the explosive on the stage of the vehicle.The designed robotic arm maintained the horizontal level of the explosive to avoid the burst and slowly laid down the explosive on the stage of the UGV (seen as Fig. 16). From Fig. 14, Fig. 15, and Fig. 16, it couldbe clearly found that the stable gripping mode of the robotic-armdesign in this study could certainly complete the task of the explosive disposition. Especially, the designed stable gripping mode help robotic arm always maintain the horizontal level of the explosive in order to keep the explosive stable to avoid the burst and reduce the casualties.



Fig 13. The robotic arm gripped and lifted up the explosive slowly, and always remained horizontal level of the explosive



Fig 14. The robotic arm remained the horizontal level during the translational motion



Fig 15. The robotic arm maintained the horizontal level of the explosive and slowly laid down the explosive on the stage of the UGV

CONCLUSION

The main purpose of this research is to construct anomnidirectional, stable UV system that integrates the mecanumwheel and robotic arm based on sensors for disaster exploration. According to the task requirements, we integrated the sensor module, core control module, motor drive module, remote control module, and robot arm module. Afterwards, we applied the dynamic information of the vehiclecollected by the sensor module to help establish the more accurate math models of the UGV and robotic arm system.In the UGV part of thedisaster-explorationUV system, the fixed-ratio control architecture in this study improved the UGV performance and advanced the handling and

flexibility of the UGV to ensure the high stability of the self-driving. Especially, when UGV encountered the obstacle unexpectedly and suddenly made an avoidance steering. UGV could always maintain the high stable driving.In addition, in the robotic arm part, through the ultrasonic and network cameras, the designed stable gripping mode of the robotic arm could certainly complete the task of the explosive disposition. Especially, the stable gripping mode help robotic arm always keep the horizontal level of the explosive to avoid the burst and keep the explosive stable to reduce the risk of blasting explosions.

Finally, we actively invested the research for disaster exploration and disaster relief and hoped this research could be an example of a good deed for others to follow. Then, throughthe researches and developments of the UVs and concerted efforts,the casualties of disasterwill be reduced in the future.

ACKNOWLEDGEMENTS

This study can be accomplished all thanks for the supports from the Ministry of Science and Technology, MOST of ROC. (MOST 106-2221-E-606-015)

REFERENCES

[1] Chi-Tang Yeh,“Research on the Development Trend and Countermeasures of Disaster Management in China in the Last Ten Years”,Taiwan,2011.

[2] Chao-Shin Lin,“Obstacle avoidance and path planning of an unm”, National Taiwan University, Taiwan Kaohsiung,2008.

[3] Jhih-Ren Wu, “ Instant obstacle detection/location and identification ”,National Success University, 2002.

[4] Chun-Chia Chen,“Self-propelled vehicle design for real-time images”, National Central University, Taiwan Taoyuan, 2007.

[5] Shih-Ta Huang,“Vision Based Tracking Control for Automatic Guided Vehicles”,National Taipei University of Technology, Taiwan Taipei, 2008.

[6] Jer-Yuan Hsu,“Drive Control and Obstacle Avoidance Planning For An Automatic Mobile Vehicle”, National Success University, Taiwan Tainan, 2002.

[7] Yi-Hong Lin,“A Study on Construction and Control of a Four-Wheel-Steer Experimental Vehicle”, National Chiao Tung University, Taiwan Hsinchu, 2008.

[8] Wu, Tung-Shin,“Experimental Studies on Obstacle Avoidance of a Four-Wheel-Steering Vehicle”, National Chiao Tung University, Taiwan Hsinchu, 2010.

[9] Wang,Po-Yao,”A Study of the Applications for the Kalman Filter on the Stably Driving Controllers of Unmanned Ground Vehicle”, National Defense University, Taiwan Taoyuan, 2013.

[10] Jhih-Hong Jian,” Predictive Analysis of Steady Steering Track of Four-wheel Vehicle”, National Taiwan University, Taiwan Taipei, 2007.

[11] Luo, Yi-Shiun,“Application of Four-Wheel Steering Control of the Vehicle Lateral Motion”, National Chiao Tung University, Taiwan Hsinchu, 2010.

[12] Yao, Chung-Chen,”Application of Four-Wheel Steering Control to Vehicle Lateral Stabilization and Rollover Prevention”, National Chiao Tung University, Taiwan Hsinchu, 2013.

[13] Yi-Hong Lin, De-Sheng Siao, Design and Implementation of Electronic Control System for Four-wheel Steering Vehicle, Issue 3, Pages 3-1 to 3-14, 2010.

[14] HUANG, KUAN-HSIEN,”The Stability Analysis and the Controller Design of the Unmanned Ground Vehicle (UGV)”, National Defense University, Taiwan Taoyuan, 2012.

[15] Chen, Ning-Qian,“The Integration and Design of the Stable Controllers for the Unmanned Ground Vehicle”, National Defense University, Taiwan Taoyuan, 2014.

[16] Da-Chao Wang, “Research and Simulation of 6-DOF Robot Arm”, Hefei University of Technology, ChinaAnhui, 2017.

[17] Hsu, Hsiang-Yung, “Control Design of Object Classification for An Intelligent Vehicle Combining Robot Arm with Computer Vision”, National Jinan International University, Taiwan Nantou, 2015

[18] Ren-Hao Wu, Kai-An You, “Industrial six-axis robotic arm”, National Taiwan University of Science and Technology, 2015.

★★★